Rare earth element-bearing tausonite and potassium barium titanates from the Little Murun potassic alkaline complex, Yakutia, Russia

ROGER H. MITCHELL

Department of Geology, Lakehead University, Thunder Bay, Ontario, Canada P7B 5E1

AND

NIKOLAI V. VLADYKIN

Institute of Geochemistry, Academy of Sciences, P.O. Box 4019, Irkutsk-33, Russia 664033

Abstract

Tausonites occurring in aegirine potassium feldspar syenite from the Little Murun potassic alkaline complex are characterised by complex growth and resorption features. These are attributed to non-equilibrium crystallisation in a dynamic environment characterised by magma mixing and/or volatile degassing. The crystals represent a transported assemblage which has no simple relationship to the magma from which their host rock crystallised. Tausonites exhibit significant normal, reverse and oscillatory compositional zoning with respect to strontium and the rare earth elements. The compositions are unique, ranging from tausonite to strontian cerian loparite, and are unlike those found in strontian perovskites from lamproites and fenites associated with carbonatites.

Compositional data are presented for Ba-rich titanates belonging to the hollandite group, $Ba(Ti,Fe)_5O_{11}$ and $K_2Ti_{13}O_{27}$. The titanates, on the basis of textural evidence, are interpreted to have formed by the reaction of K–Ba-rich residual liquids with pre-existing Ti-magnetite, ilmenite and tausonite. The compositions of the titanates are similar to those of primary titanates found in kimberlites and carbonatites.

KEYWORDS: tausonite, titanates, alkaline complex, Yakutia, Russia.

Introduction

THE Little Murun potassic alkaline complex is located at the north-western edge of the Aldan shield, south-western Yakutia (Russia), and has been described by Bilibina *et al.* (1967), Orlova (1987, 1988), and Shadenkov *et al.* (1989). The complex is notable for the occurrence of a variety of plutonic kalsilite-bearing rocks, e.g. yakutite (Smyslov 1986), effusive leucite-bearing rocks (Orlova 1987) and a wide variety of very rare minerals, e.g. charoite, tinaksite, kanasite, fedosite, etc., which have been formed in a metasomatic aureole (Vladykin *et al.*, 1983).

Recently, it has been suggested that mica-rich hypabyssal dyke rocks and the effusive leucite-bearing rocks are lamproites (Vladykin, 1985) and that the plutonic rocks are the intrusive equivalents of lamproites (Shadenkov *et al.*, 1989). In order to assess the relationships of the complex to lamproites a new mineralogical and petrological study has been initiated.

With respect to lamproites, the presence at Little Murun of tausonite ($SrTiO_3$) is of particular interest, as Mitchell and Bergman (1991) and Mitchell and Steele (1992) have noted that Sr-rich perovskites are common in lamproites. Tausonite was initially described from the Little Murun complex by Vorobyev *et al.* (1984, 1987). Few compositional data were presented, although it was recognised that some examples were relatively rare earth element-rich. During a re-examination of tausonites from the type locality at Tausonite Hill, we recognised that this mineral exhibits extraordinarily complex zoning and a compositional variation which far exceeds that reported by Vorobyev *et al.* (1987). The compositions of Little Murun perovskite reported here are unlike those of any other naturally-occurring perovskite.

Mineralogical Magazine, December 1993, Vol. 57, pp. 651–664

K–Ba-titanates were initially recognised in potassic syenites at Murun by Lazebnik *et al.* (1985) and termed priderite. Few compositional data (6 analyses) were presented by Lazebnik *et al.* (op. cit.) and unfortunately these were characterised by low analytical totals and/or represented mixtures of two titanates. Tausonite-bearing syenites examined in this work were also found to contain a number of K–Ba-titanates. Some of these titanates belong to the hollandite group of minerals and have compositional similarities to priderite, a characteristic mineral of lamproites (Mitchell and Bergman, 1991). However, others are previously unrecognised titanates or are varieties which have similarities to titanates found in group 2 kimberlites (Mitchell and Meyer, 1989) and group 1 calcite kimberlites (Mitchell, 1993*a*). The Murun occurrence represents a new paragenesis of K–Ba-titanates.

The tausonite syenite examined in this study is an allotriomorphic granular aegirine potassium feldspar syenite. The earliest minerals to crystallise included tausonite, wadeite, magnetite, ilmenite, and barytolamprophyllite. These minerals may be found included in titanite, which crystallised next as euhedral rhombic crystals or sprays of sub-parallel intergrown prisms. Titanite, in turn, was included in felt-like aggregates of green aegirine. The final minerals to crystallise were rare kalsilite and abundant potassium feldspar. Twinning was not observed in the feldspar. Early-forming minerals may also be found included in potassium feldspar and aegirine. Late-stage celsian, barium carbonate and baryte are also present.

The syenite is characterised by unusual textures. Massive aegirine aggregates possess complex fringes of small euhedral aegirine prisms that define fluidal textures. Small barytolamprophyllite prisms occur in swaths within Ba-poor potassium feldspars. These swaths encircle barytolamprophyllite-free, Ba-rich potassium feldspar, producing a texture that is similar in appearance to that of augen-gneiss. The textures suggest that the magma from which this syenite formed was extremely fluid and underwent rapid quenching upon emplacement. Tausonite syenite is one of the last intrusive rocks to have been emplaced in the complex.

Analytical methods

Perovskites were analysed by standard wavelength-dispersive methods using a Cameca SX-50 microprobe at the University of Manitoba. Synthetic and mineral standards were used for the determination of Sr and Ti ($SrTiO_3$), Fe (almandine), Mg (olivine), Mn (spessartine), Na (albite), Ca (diopside), Ba (witherite), Th (thorite), Nb (Nb_2O_5) and Ta (microlite), at an accelerating voltage of 15 kV and a beam current of 20 nA. Rare earth elements were determined using an accelerating voltage of 20 kV and a beam current of 40 nA. La and Ce were determined using $L\alpha$ lines and $LaVO_4$ and monazite standards, respectively. Pr ($L\beta$,) Nd ($L\alpha$), and Sm ($L\beta$) were determined using rare-earth-bearing glass standards prepared by Drake and Weill (1982).

As the K–Ba-titanates are too small for satisfactory electron microprobe analysis they were analysed by energy dispersive methods using a Hitachi 570 scanning electron microscope at Lakehead University. Quantitative analysis were obtained using the Tracor-Northern 'standardless' quantitative analysis package SQ. Correction factors used in this program were calibrated by analysis of ilmenite, priderite and jeppeite standards. Mitchell and Meyer (1989) have previously described the use of this technique for the analysis of K–Ba-titanates. All EDS X-ray data were obtained with an accelerating voltage of 20 kV and a beam current of 0.38 nA.

Strontium and rare earth titanates

Morphology and zoning—back scattered electron petrography. Tausonite forms large (1–2 mm) euhedral to subhedral cubic crystals that are included in potassium feldspar, aegirine and titanite, and rarely in wadeite. In transmitted light the crystals are seen to consist of a reddish-brown transparent core with a dark-red to opaque mantle.

Back-scattered electron images demonstrate that all of the crystals exhibit extraordinary complex compositional zoning, growth and resorption features. Each crystal consists of four morphologically and compositionally distinct units, referred to here as the inner and outer cores and the inner and outer mantles. Typical examples are illustrated in Figs. 1 and

The morphology of the inner and outer cores is that of a crystal form which in cross-section exhibits six crystal faces. In contrast, the inner and outer mantles appear to be cross-sections of a simple cube. The observations are interpreted to suggest that the cores have the habit of an octahedron (or icositetrahedron) and that this has been overgrown by a hexahedron.

Embayments in, and the rounded appearance of the inner cores (Fig. 1) indicates that a period of resorption occurred prior to the epitaxial overgrowth of the outer cores. Resorption of the

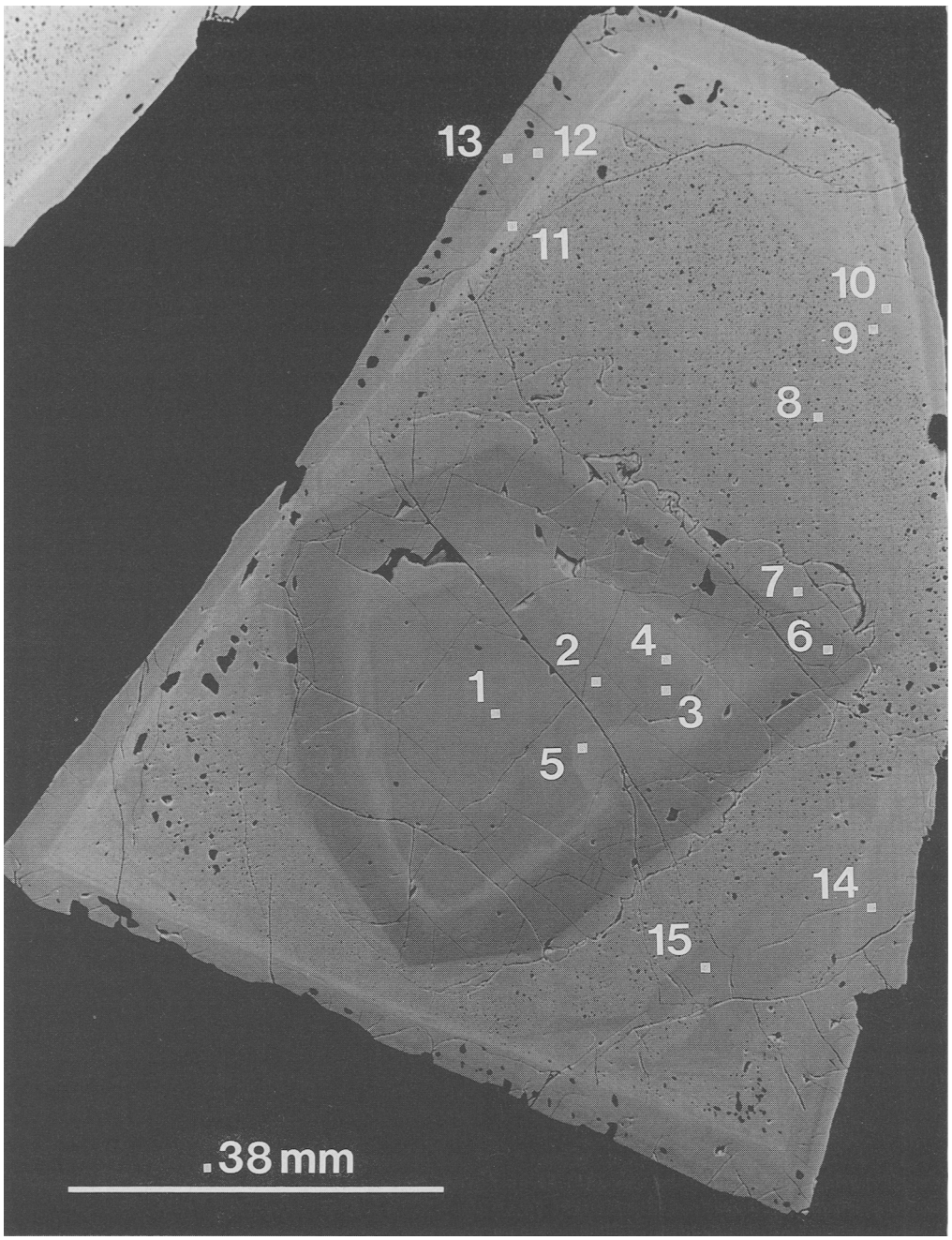

FIG. 1. Back scattered electron image of a zoned tausonite crystal characterised by an angular unresorbed core. Note the complex zoning and domain structures in the inner mantle of a tausonite crystal, and the presence of oscillatory zoning in the epitaxial outer mantle.

core occurred, in some instances, prior to the growth of the mantle. All stages in the resorption process can be found; ranging from no resorption (Fig. 1) to strongly resorbed rounded cores (Fig.

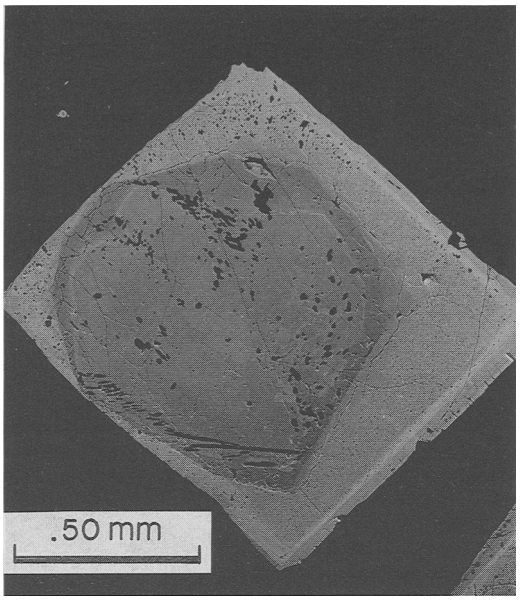

FIG. 2. Back scattered electron image of a zoned tausonite crystal characterised by a resorbed core.

2). Tausonites with cores exhibiting radically different degree of resorption, occur side-by-side.

The outer cores were subsequently overgrown by the inner mantle. This is now characterised by numerous resorption pores of widely varying size (Figs. 1 and 2) together with complex irregular domains (see below). The outer mantle, which grew epitaxially upon this substrate, exhibits oscillatory zoning, and typically consists of at least two-to-four compositionally distinct zones lacking resorption pores.

Back scattered electron images (Figs. 1 and 2) of the inner cores suggest that they exhibit relatively little compositional variation and are of slightly higher average atomic number (AZ) than the bulk of the outer core. The outer core, in contrast, is very strongly zoned. The region immediately overlying the inner core consists of high AZ material. This grades by continuous and/or discrete compositional variation, reflecting decreasing AZ, towards the low AZ outer core margin.

The inner mantle consists principally of uniform high AZ material (Figs. 1 and 2). Typically, and especially, in the outer margins there occur complex intergrowths and domains of material of lower AZ (Figs. 1 and 3). This material forms bands and irregular masses which commonly exhibit no particular orientation. Many of the irregular domains of lowest AZ have the appearance of clasts (Figs. 1 and 3). Rarely, thin elongate zones of low AZ form sub-parallel arrays suggestive of exsolution textures (Fig. 3). Typically, these lower AZ replacements lack the resorption pores which characterise the bulk of the inner core, suggesting that pore formation occurred prior to their formation. The irregular low AZ zones are interpreted to have formed prior to the outer mantles (see below) as material forming the latter truncates them.

The outer mantles (Figs 1–3) consist of a series of thin epitaxial compositionally-diverse zones. These typically lack resorption pores. The majority of the bands are relatively uniform in composition, although rarely within-band irregular domains of material of differing AZ may be observed (Figs. 1 and 3).

Compositional variation. All tausonite crystals examined exhibit extensive compositional variation with respect to Sr (26.2–50.07 wt.% SrO) and rare earth element (0.1–9.8 wt.% Ce_2O_3) contents and relatively little variation in Ca content (1.9-5.5 wt.% CaO). Other elements present in significant amounts include Na_2O (0.5–3.4 wt.%), Nb_2O_5 (0.0–1.28 wt.%), ThO_2 (0.0–2.7 wt.%) and BaO (0.3–1.2 wt.%). All tausonites contain less than 0.5 wt.% FeO and negligible MnO and MgO (<0.05 wet.%).

Table 1 presents data for the extremes of the range of compositions encountered. Recalcula-

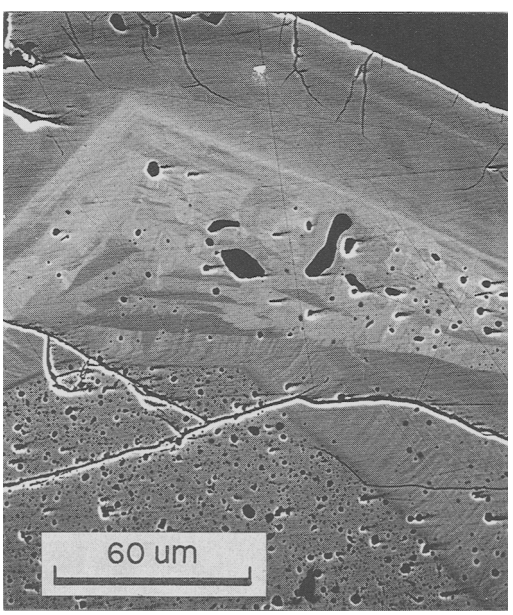

FIG. 3. Back scattered electron image showing resorption pores, complex zoning and domain structures in the inner mantle of a tausonite crystal.

Table 1. Representative tausonite compositions.

	Wt.% oxides		Cations/3 oxygens			Mol% Components		
	1	2		1	2		1	2
ThO_2	0.0	2.00	Th	-	0.013	LUESHITE	0.21	0.15
La_2O_3	0.68	6.34	La	0.007	0.069	LOPARITE	5.05	37.41
Ce_2O_3	1.23	9.59	Ce	0.014	0.103	$CaNb_2O_6$	0.0	0.0
Pr_2O_3	0.06	0.54	Pr	0.001	0.006	$BaTiO_3$	0.68	0.58
Nd_2O_3	0.31	1.30	Nd	0.003	0.014	PEROVSKITE	7.27	11.04
Sm_2O_3	0.0	0.04	Sm	-	0.000	TAUSONITE	86.79	49.83
SrO	49.40	27.78	Sr	0.862	0.475			
CaO	2.24	3.33	Ca	0.072	0.105	% cations not assigned		
BaO	0.57	0.48	Ba	0.007	0.006	A-site	0.73	2.80
Na_2O	0.59	3.31	Na	0.034	0.189	B-site	1.10	5.02
			A =	1.000	0.980			
Nb_2O_5	0.15	0.79	Nb	0.002	0.011			
Ta_2O_5	0.0	0.05	Ta	-	0.000			
TiO_2	44.03	44.48	Ti	0.997	0.986			
FeO	0.19	0.26	Fe	0.005	0.006			
MnO	0.04	0.0	Mn	0.001	-			
MgO	0.0	0.0.	Mg	-	-			
	99.49	100.29	B =	1.004	1.003			

Total Fe calculated as FeO.

tion of the data into end-number perovskite group compounds (ABO_3; where A = Ca, Sr, Ba, Th, *REE* and B = Ti, Fe, Nb, Ta, Mn, Mg) demonstrates that the tausonites are essentially members of the loparite-tausonite ($Na_{0.5}$-$Ce_{0.5}TiO_3$–$SrTiO_3$) solid solution series and that only limited solid solution towards perovskite ($CaTiO_3$) is present. In the recalculation procedure all *REE* are treated as forming compounds that are isomorphous with loparite. Low Ba, Nb and Na contents are reflected in the presence of less than 1 mol.% of the $BaTiO_3$ and lueshite ($NaNbO_3$) and members. Cations not assigned to end-member molecules account for less than 5% of the total A or B-site cations. The majority of these represent excess Ti in the B-site and A-site cations such as Th, which cannot easily be assigned to any real or hypothetical perovskite type compounds.

Fig. 4 illustrates the range of compositions encountered in Murun tausonites, in terms of the ternary perovskite–loparite–tausonite system, and indicates that the majority of the minerals are best termed cerian calcian tausonite and calcian-tausonite. Very few compositions plot in Fig. 4 as tausonite *sensu stricto* (i.e. >90 mol.% $SrTiO_3$).

Tausonite compositions reported by Vorobyev *et al.* (1987) are also plotted in Fig. 4. These limited data fall into two groups designated tausonite 1 and 2 by Vorobyev *et al.* (op. cit.). Tausonite 1 corresponds to *REE*-poor tausonite and tausonite 2 to cerian tausonite. Vorobyev *et -al.* (op. cit.) did not investigate the extensive compositional zoining found in the Little Murun tausonite and their two groups are merely parts of the wide continuum of compositions recognised in this work.

Fig. 5 and Table 2 illustrate the compositional variation encountered in the tausonite crystal depicted in Fig. 1. These data are representative of the compositional zonation found in all other crystals examined. The inner core is Sr-rich and *REE*- and Na-poor (anals. 1–3). The ThO_2 (<0.2 wt.% and Nb_2O_5 (0.5 wt.%) and BaO (<0.7 wt.%) contents are all low. The outer core shows continuous compositional variation from a rela-

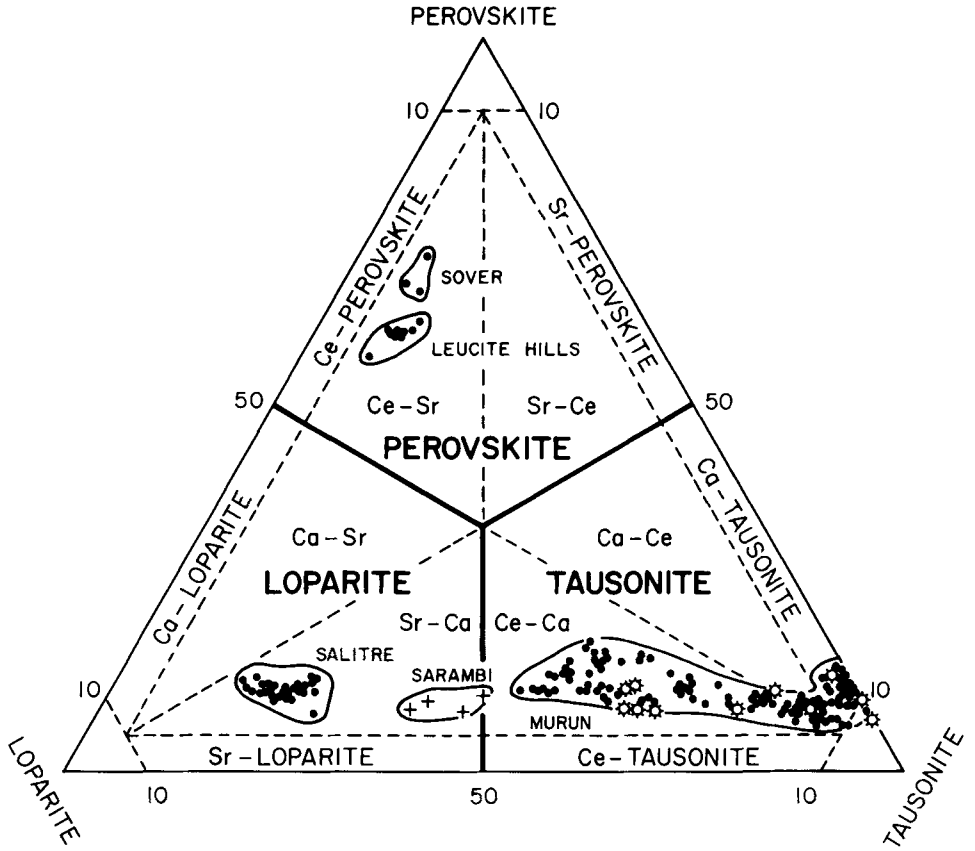

FIG. 4. Compositions (mol.% end-member molecules) of tausonites from Little Murun and other Sr-bearing perovskites plotted in the ternary system perovskite–loparite–tausonite. Data sources: Salitre, and Sover (this work), Sarambi (Haggerty and Mariano, 1983), Leucite Hills (Mitchell and Steele, 1992). Tausonite compositions given by Vorobyev *et al.* (1987) are indicated by *.

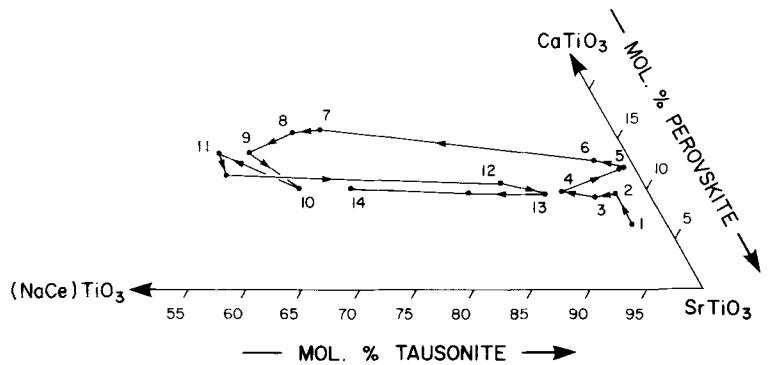

FIG. 5. Compositional zoning trends (mol.% end-member molecules) occurring within the tausonite crystal illustrated in Fig. 1. Analysis points (1–14) correspond with compositions listed in Table 2.

Table 2. Compositional variation of a zoned tausonite

	1	2	3	4	5	6	7	8	9	10	11	12	13	14	15
TiO_2	43.69	44.15	43.68	44.19	43.69	44.83	44.30	44.61	43.87	43.79	44.04	44.11	44.20	44.25	44.66
FeO	0.24	0.18	0.24	0.16	0.19	0.13	0.27	0.26	0.46	0.30	0.44	0.08	0.15	0.28	0.39
MnO	0.04	0.0	0.0	0.0	0.0	0.0	0.0	0.0	0.0	0.0	0.0	0.0	0.0	0.0	0.0
CaO	1.34	2.89	2.81	2.99	2.65	3.91	4.95	4.68	4.07	2.95	4.09	3.17	2.92	2.55	5.08
MgO	0.0	0.0	0.0	0.0	0.0	0.0	0.0	0.0	0.0	0.0	0.0	0.0	0.0	0.0	0.0
Na_2O	0.50	0.61	0.61	0.74	0.79	0.69	2.31	2.59	2.83	2.50	3.11	1.16	0.90	2.23	2.45
BaO	0.54	0.67	0.63	0.77	1.04	0.98	0.50	0.74	0.65	0.50	0.67	0.72	0.86	0.29	0.55
SrO	49.23	48.43	48.17	45.92	46.51	46.74	33.47	31.21	29.04	32.61	28.09	43.18	45.87	34.60	31.62
ThO_2	0.13	0.0	0.19	0.07	0.0	0.0	0.94	0.95	1.47	2.09	1.16	1.05	0.28	1.88	0.95
La_2O_3	0.52	0.39	0.69	0.97	1.29	0.35	3.81	4.63	5.34	5.06	5.78	1.32	0.76	4.22	4.25
Ce_2O_3	0.72	0.63	1.19	1.80	1.86	0.76	6.21	7.69	8.84	7.92	9.53	2.97	2.27	7.01	7.27
Pr_2O_3	0.05	0.03	0.14	0.13	0.10	0.08	0.41	0.51	0.52	0.45	0.55	0.25	0.24	0.47	0.46
Nd_2O_3	0.12	0.19	0.15	0.38	0.34	0.24	1.11	1.25	1.26	1.23	1.34	0.77	0.74	1.13	1.19
Sm_2O_3	0.04	0.0	0.0	0.0	0.0	0.0	0.03	0.06	0.0	0.08	0.10	0.02	0.01	0.06	0.13
Nb_2O_5	0.13	0.37	0.48	0.32	0.68	0.0	0.61	0.75	0.71	0.48	0.83	0.38	0.46	0.53	0.75
Ta_2O_5	0.09	0.20	0.08	0.05	0.20	0.0	0.04	0.06	0.13	0.0	0.06	0.08	0.10	0.02	0.0
	97.98	98.74	99.06	98.49	99.34	98.71	98.96	99.99	99.13	99.96	99.79	99.26	99.76	99.92	99.98

Total Fe calculated as FeO; 0.0 = below detection limit; see figure 5 for analysis positions.

tively *REE*-rich region (anals. 4 and 5) adjacent to the inner core, to Sr-rich, *REE*-poor margins (anal. 6). The outer core is Ba-rich relative to the inner core.

The inner mantle is Na-, Th-, Nb-, and *REE*-rich relative to the inner and outer cores (anals. 7–10), reflecting increased solid solution towards loparite-rich tausonites. All of these elements increase by continuous compositional zonation towards the margins of the inner mantle. Domains of lower AZ within the porous tausonite contain less *REE* and more CaO (anal. 15) than their hosts. The trend of *REE*-enrichment culminates in the first discrete epitaxial zone of the outer mantle (anal. 11). Subsequently-formed epitaxial overgrowths are thin zones of low or high *REE* tausonite (anals. 12–14), although *REE*-contents never exceed the levels found in the first zone.

Perovskite-group minerals having compositions similar to the loparite–tausonite solid solutions documented above, have not previously been reported. Only perovskites from rheomorphic fenites adjacent to the Sarambi and Chiriguelo (Paraguay) carbonatite complexes (Haggerty and Mariano, 1983), approach the compositions of the Murun perovskites. Fig. 4 shows that Sarambi/Chiriguelo perovskites are *REE*-rich and Sr-poor relative to Murun tausonites and are essentially strontian calcian loparites.

Relatively strontium-poor loparites were also described by Haggerty and Mariano (op. cit.) in rheomorphic fenites from the Salitre-1 (Brazil) carbonatite complex. Material from this locality was re-examined during the course of this work. The loparites occur as small (20–100 μm) subhedral to euhedral crystals of hexahedral habit. Back-scattered electron imagery shows that individual grains are relatively homogeneous, although a few occasionaly contain small irregular domains of higher AZ. New compositonal data (52 analyses) for perovskites from this occurrence (Table 3) demonstrate that the suite as a whole exhibits a limited range in composition (SrO = 6.8–13.2 wt.%; Ce_2O_3 = 12.7–17.9 wt.%; Na_2O = 6.4–8.1 wt.%) and has low Ca contents (2.8–3.6 wt.% CaO). They differ principally from the Murun tausonites in containing less Sr and more Na and *REE*, reflecting their dominantly loparitic composition. They differ further, in that they contain substantial amounts of Nb, with the majority containing 5.5–8.4 wt.% Nb_2O_5, while domains of higher AZ are enriched in Nb_2O_5 (11.5–14.5 wt.%). These domains are also enriched in ThO_2 (4.7–6.2 wt.%) relative to the low Nb portions of the crystal (ThO_2 = 0.5–1.9 wt.%). The enrichment in Nb indicates that these perovskites are members of a quaternary solid-solution series between perovskite, lueshite, tausonite and

loparite (Table 3, anals. 1–5) and are best described as niobian strontian loparite. Fig. 4 illustrates their composition projected into the perovskite–loparite–tausonite ternary for comparison with other Sr-rich perovskites. The overall compositional variation shown by perovskites from Murun, Sarambi and Salitre suggests that a continuous solid solution exists between loparite and tausonite.

An occurrence of *REE*-, Sr-rich perovskite has been described from the Leucite Hills lamproites by Mitchell and Steele (1992). These perovskites are poor in *REE*, Na and Sr, relative to those described above as they are essentially cerian strontian perovskites (Fig. 4, Table 3 anals. 6–7). Sr-perovskites occurring in the Sover North group 2 kimberlite (this work) are also of similar composition (Table 3, anals. 8–9). Although the database is limited, Fig. 4 may be interpreted to suggest that natural examples of the solid-solution series between perovskite and tausonite may not occur.

Potassium and barium titanates

Potassium and barium titanates belonging to three compositionally distinct groups occur occasionally in the tausonite-bearing syenite. They occur principally as subhedral prisms and anhedral grains mantling earlier-formed tausonite or Ti-magnetite. Less commonly, they are found as discrete small (<5 μm) subhedral crystals enclosed in groundmass potassium feldspar. The paragenesis is interpreted to indicate that the majority of the K-Ba titanates are the products of reaction between pre-existing titanates and the groundmass-forming magma. They do not appear to have crystallised as liquidus phases. All of these titanates occur as very small (<10 μm) crystals. Their size and the difficulty of separating them from intergrown phases unfortunately precludes X-ray diffraction studies.

K-Ba-hollandites. The most abundant potassium-bearing Ba-rich titanates contain 0.2–2.0 wt.% K_2O, 8.7–14.4 wt.% Fe_2O_3 and 11.5–21.1 wt.% BaO. Representative compositions are given in Table 4. Individual crystals may be zoned or homogenous. Calculation of structural formulae on the basis of 16 oxygens suggests that the minerals probably belong to the hollandite group of titanates and are essentially solid solutions between $BaFe^{2+}Ti_7O_{16}$ and $BaFe_2^{3+}Ti_6O_{16}$. The small amount of potassium present indicates limited solid solution towards analogous K-based septa- and hexatitanates.

Lazebnik *et al.* (1985) have previously reported the presence of titanates of similar composition at Murun and termed them priderite. However, Table 4 demonstrates that Murun Ba–Fe-titanate commonly has less than 7 atoms Ti/16 oxygens and contains more Fe (>10.8 wt.% total Fe calculated as Fe_2O_3) than ideal (K, Ba)-Fe septatitanates comprising the priderite series (Mitchell and Meyer, 1989). Only the titanates with the least Fe contents (Table 4, anals. 3–4) have structural formulae which accord with $BaFe^{2+}Ti_7O_{16}$. Estimation of the relative proportions

Table 3. Representative compositions of Sr-perovskites from Salitre 1 (Brazil), Middle Table Mountain, Leucite Hills (Wyoming) and Sover North (South Africa)

	1	2	3	4	5	6	7	8	9
TiO_2	42.09	29.74	40.43	37.52	37.75	50.1	50.4	55.4	55.0
FeO	0.09	0.49	0.57	0.14	0.17	0.72	0.4	2.4	1.0
MnO	0.0	0.0	0.0	0.0	0.0	0.0	0.0	0.0	0.0
CaO	3.03	2.87	3.62	3.08	3.03	21.1	23.3	22.3	22.2
MgO	0.0	0.0	0.0	0.0	0.0	0.0	0.0	0.0	0.0
Na_2O	6.81	6.92	6.69	7.85	8.09	3.01	2.89	2.4	1.9
BaO	0.0	0.0	0.0	0.0	0.0	0.26	0.33	0.0	0.0
SrO	8.86	10.62	11.65	7.55	6.95	5.53	7.19	4.5	4.5
ThO_2	1.21	0.79	0.71	4.67	6.19	0.0	0.0	0.0	0.0
La_2O_3	11.25	10.39	9.30	10.05	8.26	4.14	3.56	3.3	5.3
Ce_2O_3	16.94	16.56	15.26	15.41	12.74	9.26	7.50	6.3	8.4
Pr_2O_3	0.71	0.87	0.84	0.93	0.78	0.87	0.76	n.d	n.d
Nd_2O_3	2.06	2.37	2.51	2.05	1.89	2.61	2.52	2.9	1.4
Sm_2O_3	0.02	0.10	0.07	0.01	0.12	0.15	0.22	n.d	n.d
Nb_2O_5	6.49	7.59	8.28	11.52	14.17	0.69	1.19	0.4	0.4
Ta_2O_5	0.28	0.42	0.29	0.11	0.00	0.0	0.0	n.d	n.d
	99.84	99.73	100.22	100.89	100.14	98.44	100.26	99.99	100.0
Mol. % end member molecules									
LUESHITE	9.5	10.9	11.4	15.9	20.6	0.5	0.8	0.4	0.3
LOPARITE	64.2	61.7	56.2	60.7	55.9	31.0	28.1	25.6	20.2
PEROVSKITE	10.2	9.5	11.8	10.0	10.6	60.1	60.1	66.6	66.6
TAUSONITE	16.1	18.9	20.6	13.4	12.9	8.5	11.0	7.4	7.3

1-5 Salitre-1 (this work); 6-7 Middle Table Mountain (Mitchell and Steele 1992); 8-9 Sover North (this work); Total Fe calculated is FeO; 0.0 = below detection limit.

Table 4. Representative compositions of Ba-Fe-hollandites from the Murun tausonite syenite and the Sover North kimberlite.

	1	2	3	4	5	6	7	8	9
Nb_2O_5	0.0	0.0	0.0	0.0	0.0	1.4	1.5	0.6	1.2
TiO_2	69.7	67.2	72.3	69.0	63.5	72.1	70.2	68.7	67.3
V_2O_3	0.0	0.0	0.0	0.0	0.0	0.7	0.9	1.3	1.2
Fe_2O_3	12.8	14.4	11.8	11.4	12.4	10.0	10.2	12.0	10.1
MnO	0.0	0.5	0.0	0.4	1.3	0.0	0.0	0.0	0.0
MgO	1.1	0.0	0.0	0.0	0.0	0.6	0.0	0.0	0.3
K_2O	1.1	0.3	0.6	0.6	0.2	1.1	0.7	0.4	0.3
BaO	14.2	16.7	15.1	18.0	20.5	14.8	16.2	17.1	19.6
	98.9	99.1	99.8	99.4	98.5	98.7	98.2	99.5	98.8
Structural formulae based on 16 oxygens									
Nb	-	-	-	-	-	0.079	0.086	0.034	0.070
Ti	6.581	6.483	6.764	6.660	6.374	6.742	6.667	6.555	6.543
V	-	-	-	-	-	0.069	0.090	0.131	0.123
Fe	1.210	1.391	1.105	1.101	1.246	0.936	0.969	1.146	0.983
Mn	-	0.054	-	0.044	0.147	-	-	-	-
Mg	0.206	-	-	-	0.119	-	-	-	0.058
K	0.176	0.049	0.095	0.098	0.034	0.174	0.113	0.065	0.049
Ba	0.699	0.841	0.747	0.906	1.073	0.721	0.802	0.850	0.993

Total Fe calculated as Fe_2O_3. 1-5 Murun, 6-9 Sover North.

of Fe^{2+} and Fe^{3+} is impossible due to the non-stoichiometric character of hollandites (Mitchell and Meyer, 1989; Myrha *et al.*, 1988). The solid solution towards Ba–Fe^{3+}-hexatitanate suggests that these minerals should not be referred to as priderites (Mitchell and Meyer, 1989).

Fig. 6 demonstrates that Ba-Fe titanates from Murun are poor in K_2O compared with priderites from the Leucite Hills and West Kimberley lamproites. Priderites from the Leucite Hills exhibit a similar range in BaO content to the Murun hollandites. Fig. 6 shows that both groups of hollandites exhibit a compositional trend away from ideal Ba-based septa- and hexatitanates. This trend is a reflection of non-stoichiometry in the 8-fold tunnel site occupied by Ba and K. Murun hollandites differ from Leucite Hills hollandites in that the latter commonly contain appreciable Cr_2O_3 (up to 6 wt.%; Mitchell and Bergman, 1991).

Ba–Fe-titanates in a reaction association with potassium titanate (see below) have thus far only been recognised in the Sover North (South Africa) group 2 kimberlite (this work). This kimberlite represents a highly evolved fraction of a group 2 kimberlite or orangeite magma (Mitchell, 1993*b*) and is characterised by the presence of groundmass potassium feldspar and potassium richterite. In these rocks Ba–Fe-titanates mantle earlier-formed potassium titanates in a manner analogous to that observed at Murun. Table 4 and Fig. 6 show that these hollandites have similar compositions to those from Murun. They differ in having appreciable Nb_2O_5 and V_2O_3 contents.

Ba–Fe-hollandites, not associated with potassium titanate, but of similar composition to the Murun and Sover North hollandites, are also known from the Wesselton and Benfontein (South Africa) kimberlite sills (Mitchell, 1993*a*), the Prairie Creek (Arkansas) lamproite (Mitchell and Bergman, 1991) and the Kovdor (Russia) carbonatite (Zhuravleva *et al.*, 1978). Of these occurrences, only the Kovdor hollandites appear to have been formed by reactions with pre-existing Ti-minerals. In contrast, kimberlite and lamproite hollandites appear to be primary liquidus phases. Fig. 6 shows that Wesselton and Benfontein hollandites exhibit a similar range in Ba/K ratios to those from Murun. They differ characteristically in containing no K but appreciable Nb or V (Mitchell, 1992*a*).

Fe-bearing barium titanate. A titanate that is Ba-rich and Fe-poor relative to Ba–Fe-hollandite is found intergrown with this mineral and as discrete reaction mantles upon magnetite. The principal compositional variation is with respect to Fe which replaces Ti while Ba remains relatively constant (Table 5). The content of K is particularly low and compositions therefore plot on or near the $BaO–TiO_2$ join in Fig. 6. Calculation of the structural formula on the basis of 5 oxygens (Table 5) suggests that the mineral has the composition (K, Ba) $(Fe, Ti)_5O_{11}$. The monoclinic compound, $BaTi_5O_{11}$, has been synthesised by Tillmans (1969) and Ritter *et al.* (1986) but has not previously been reported as a mineral.

Potassium titanate. A Ba-free potassium titanate mantled by hollandite occurs in both the Murun tausonite syenite and the Sover North group 2 kimberlite. Representative compositions are given in Table 6. Lazebnik *et al.* (1985) have previously reported the presence of this mineral at Murun and termed it priderite. Mitchell and

Meyer (1989) found discrete anhedral crystals of similar composition to these potassium titanates in the Star group 2 kimberlite. These latter minerals differ in containing appreciable contents

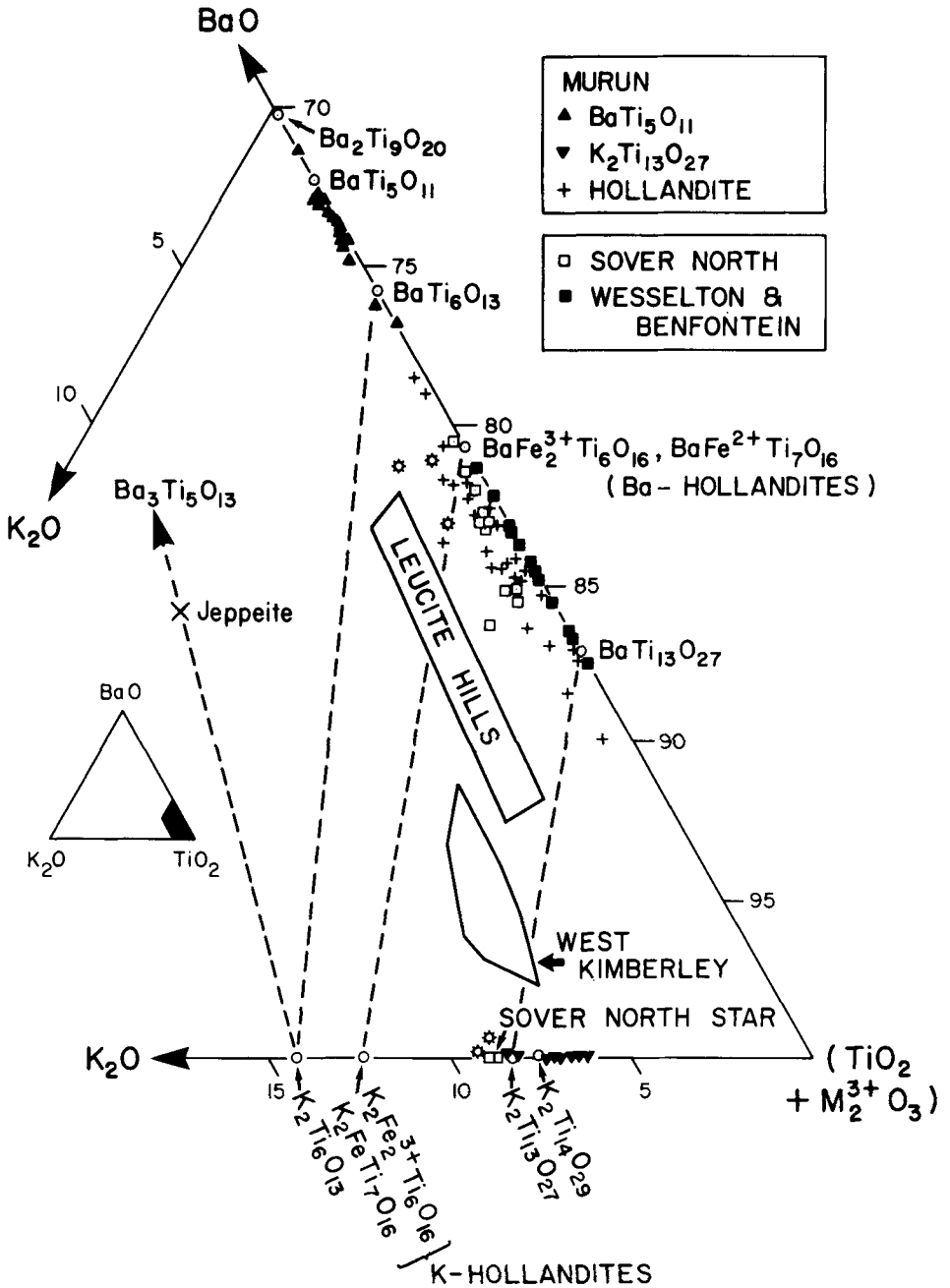

FIG. 6. Compositions (wt.%) of K–Ba-titanates plotted in the ternary system K_2O–BaO–(TiO_2 + Fe_2O_3 + V_2O_3 + Nb_2O_5). Data sources; Murun[+] (this work), Murun[*] (Lazebnik *et al.*, 1985), Benfontein and Wesselton (Mitchell, 1993*a*), Sover North (this work), Star (Mitchell and Meyer, 1989), Leucite Hills and West Kimberley priderites (Mitchell, unpub. data), jeppeite (Mitchell and Bergman, 1991).

of V_2O_3 (1–5 wt.%), Cr_2O_3 (0.5–2.0 wt.%) and Nb_2O_5 (1–7 wt.%). Mitchell and Meyer (1989) considered the minerals to be Nb-bearing potassium analogues of mannardite ($BaV_2Ti_6O_{16}$), and thus members of the hollandite group.

Fig. 6 demonstrates that the Murun and Sover North potassium titanates contain more TiO_2 (>76.3 wt.%) and less K_2O (< 12.9 wt.%) than expected, if the mineral was the $K_2FeTi_7O_{16}$ member of the priderite series. All of the Sover North compositions plot close to ideal $K_2Ti_{13}O_{27}$. Structural formulae (Table 6) are in agreement with this stoichiometry. Some of the Murun potassium titanates have this composition; however, others are deficient in K and are best regarded as non-stoichiometric varieties. These low K samples do not recalculate as any other acceptable compounds in the system K_2O–TiO_2. Recalculation of the data on the basis of 16 oxygens demonstrates that the minerals are unlikely to be hollandites as they are deficient in *A*- and *B*-site cations i.e. K = 0.9–1.2 and Fe <0.8 atoms/16 oxygens. Reconsideration of the nature of the Star potassium titanates suggests that they too should be regarded as Nb- and V-bearing varieties of $K_2Ti_{13}O_{27}$ rather than hollandites.

Table 5. Representative compositions of barium titanate from the Murun tausonite syenite

	1	2	3	4	5
TiO_2	68.3	66.2	66.7	61.8	73.26
Fe_2O_3	3.6	5.8	6.5	11.6	-
MnO	0.0	0.6	0.0	0.7	-
MgO	0.0	0.0	3.62	0.0	
K_2O	0.3	0.0	0.0	0.3	-
BaO	26.9	26.9	26.4	25.0	27.74
	99.1	99.5	99.7	99.4	
Structural formulae based on 11 oxygens					
Ti	4.798	4.665	4.667	4.376	
Fe	0.256	0.410	0.454	0.822	
Mn	-	0.050	-	0.056	
Mg	-	-	-	-	
K	0.036	-	0.017	0.036	
Ba	0.986	0.990	0.960	0.924	

Total Fe calculated as Fe_2O_3. 1-4 Murun; 5 ideal composition of $BaTi_5O_{11}$. 0.0 = below detection limit.

Discussion

The Sr-perovskites described above have no textural or compositional counterparts. The enrichment in Sr far exceeds that reported in other parageneses of Sr-bearing perovskites.

The zoning and resorption features exhibited by the tausonites are not easily explained but it is reasonable to relate many of these features to crystal transport and magma movement (Anderson, 1984) and/or growth kinetics (Bottinga *et al.*, 1966).

Zoning within the cores is symmetrical and 'stratigraphically' continuous (Figs. 1 and 2). Bottinga *et al.* (op. cit.) have suggested that such zoning in plagioclase reflects changes in the bulk composition of the magma. This hypothesis may be satisfactory in cases in which the zoned minerals are major components of the mineral assemblage crystallising from a magma. However, it is difficult to envisage how changes in the bulk composition of the magma that drastically change the Sr and *REE* contents of tausonite would not be reflected in other minerals in the tausonite-bearing syenite. In fact, only the tausonites are strongly zoned, suggesting that they either grew in a magma which is unrelated to that from which their current host rock crystallized, or

Table 6. Representative compositions of potassium titanates from the Murun tausonite syenite and the Sover North kimberlite.

	1	2	3	4	5	6	7	8	9
Nb_2O_5	0.0	0.0	0.0	0.0	0.0	1.0	1.1	0.9	-
TiO_2	86.0	87.0	84.1	83.5	83.9	83.1	82.3	81.9	91.69
V_2O_3	0.0	0.0	0.0	0.0	0.0	0.6	0.7	0.9	-
Fe_2O_3	4.8	5.4	7.5	8.4	8.8	6.4	6.9	7.4	-
MnO	0.0	0.0	0.3	0.0	0.0	0.0	0.0	0.0	-
MgO	0.0	0.0	0.0	0.0	0.0	0.0	0.0	0.3	-
K_2O	8.5	7.4	7.0	7.2	6.7	8.5	8.8	8.5	8.31
BaO	0.0	0.0	0.0	0.0	0.0	0.0	0.0	0.0	-
	99.3	99.8	98.9	99.1	99.4	99.9	99.8	99.9	
Structural formulae based on 27 oxygens									
Nb	-	-	-	-	-	0.089	0.100	0.082	
Ti	12.456	12.469	12.236	12.150	12.134	12.087	11.998	11.914	
V	-	-	-	-	-	0.088	0.111	0.144	
Fe	0.696	0.774	1.092	1.223	1.275	0.928	1.001	1.074	
Mn	-	-	-	-	-	-	-	-	
Mg	-	-	-	-	-	-	-	0.081	
K	2.088	1.799	1.777	1.728	1.644	2.101	2.163	2.101	
Ba	-	-	-	-	-	-	-	-	

Total Fe calculated as Fe_2O_3. 1-5 Murun, 6-8 Sover North; 9 ideal composition of $K_2Ti_{13}O_{27}$; 0.0 = below detection limit.

that the zoning does not reflect changes in bulk composition. We consider that both factors may be involved.

Accordingly, we suggest that normal equilibrium growth of the slightly zoned inner cores was interrupted by a change in *P–T–X* conditions. Increases in temperature due to magma mixing or changes in volatile contents may have removed the tausonite from its stability field. In either case a hiatus in crystallisation, in some instances followed by resorption, would subsequently occur.

Formation of the strongly reversed-zoned (i.e. *REE* depletion) outer cores is best ascribed to non-equilibrium crystallisation at rapidly growing surfaces where steep diffusional gradients and local supersaturation lead initially to the preferential crystallisation of loparitic perovskite. Crystallisation may have been initiated by rapid cooling, caused perhaps by transport of the seed crystals (Anderson, 1984).

Truncated growth zoning and resorption features at the core–mantle boundaries indicate that crystallisation conditions changed significantly prior to the formation of the mantles. As suggested above, transport of crystals and/or magma mixing are the only feasible mechanisms for inducing such a hiatus in crystallisation. Subsequently, growth conditions were established again and the continuous normally-zoned, i.e. a trend of *REE* enrichment, inner core was formed. The change in growth form indicates significant changes in temperature and the absence of oscillatory or crystallographically controlled zoning suggests that kinetic factors were not important in the formation of this portion of the crystal. The significant change in composition relative to the core may reflect crystallisation in liquid of differing bulk composition.

The presence of abundant resorption pores indicates that resorption of the inner core occurred prior to the formation of the irregular domains in the outer parts of the inner mantle. The origin of these domains remains obscure and it is unclear whether they represent growth or resorption features. The absence of any crystallographic control on their disposition suggests that they are not simple resorption features. The domains have some similarity to 'patchy zones' described by Anderson (op. cit.). These were found between oscillatory growth bands in plagioclase and are considered by Anderson (op. cit.) to be growth features formed from supersaturated liquids. Subsequent to their formation, further resorption of the inner mantle occurred before deposition of the outer mantle.

The final crystallisation stage in the growth of the tausonite crystals is represented by the outer mantles which are characterised by oscillatory zoning similar to that observed in feldspars. Following Anderson (op. cit.), we suggest that this zoning probably originated from non-equilibrium crystallisation in a turbulent environment.

Tausonite formation is thus considered to be a complex cycle of growth and resorption. The bulk of the tausonite probably formed in a turbulent magma chamber where mixing and/or degassing led to alternating conditions of oversaturation and undersaturation. We conclude that the tausonite crystals represent a transported assemblage which have no simple relationship to their current hosts.

The K–Ba-titanates, on the basis of textural evidence, do not appear to be primary liquidus phases. They appear to have formed where residual K- and Ba-rich magma has reacted with previously crystallised tausonite and magnetite.

Although detailed discussion of the affinities of the Muran syenites with lamproites is beyond the scope of this paper, some comment upon this topic is called for, given the unusual nature of the

Table 7. Representative compositions of minerals in tausonite syenite.

	1	2	3	4	5	6	7	8
SiO_2	28.68	29.62	45.91	51.27	51.65	29.72	63.49	n.d.
TiO_2	25.69	27.29	0.50	0.48	0.43	40.80	0.0	53.12
ZrO_2	0.02	0.03	32.77	n.d.	n.d.	n.d.	n.d.	n.d.
Al_2O_3	0.20	0.16	0.0	0.24	0.19	0.01	17.98	n.d.
FeO*	5.76	5.19	0.04	30.67	30.79	1.42	1.14	25.34
MnO	1.68	1.59	0.0	0.20	0.20	0.10	0.0	21.09
MgO	0.19	0.22	0.0	0.57	0.50	0.0	0.0	0.0
CaO	1.00	1.04	0.0	2.56	1.92	25.57	0.0	n.d.
SrO	7.60	10.21	0.0	n.d.	n.d.	n.d.	n.d.	n.d.
BaO	17.32	14.93	0.0	0.14	0.0	0.19	2.67	n.d.
Na_2O	7.79	7.16	0.0	12.16	12.39	0.45	0.15	n.d.
K_2O	3.07	2.96	21.90	0.08	0.05	0.0	14.76	n.d.
	99.00	100.40	101.12	98.37	98.12	98.26	100.19	99.55

*Total Fe calculated as FeO; 1-2 barytolamprophyllite; 3 wadeite; 4-5 aegirine; 6 sphene; 7 potassium feldspar; 8 Mn-ilmenite. n.d. = not determined; 0.0 = below detection limit.

mineral assemblage present. The tausonite-bearing aegerine syenite has some similarities to lamproites in that hollandite-group minerals coexist with wadeite and potassium feldspar. The latter two minerals have compositions (Table 7) similar to those of wadeites and potassium feldspars in lamproites. The presence of barytolamprophyllite, titanite and aegirine (Table 7) is not a characteristic of lamproites. However, the *P–T–X* conditions of the tausonite syenite may be such that the barytolamprophyllite may proxy for shcherbakovite, as this mineral is known to coexist with wadeite in other Murun syenites.

Evidence against an affinity with lamproites is that similar assemblages, e.g. strontian-loparite, lamprophyllite (20.7 wt.% SrO, 0.7 wt.% BaO), potassium feldspar and aegirine occur in rheomorphic fenites associated with carbonatites (Haggerty and Mariano, 1983). These occurrences differ in that they contain chevkinite and nepheline, and lack wadeite.

Hollandite-group K–Ba-titanates are now known from a variety of parageneses including carbonatites, calcite kimberlites, and group 2 kimberlites (orangeites). The only common factors in their genesis appears to be low temperatures and high contents of K and Ba in the parent magmas. Mitchell and Bergman (1991) caution that the mere presence of K-Ba-titanates cannot be used to infer magma affinities without consideration of their composition, the total paragenesis and the nature of comagmatic antecedents.

Thus, although the mineral assemblage of tausonite syenite suggests some affinities with lamproites, there are also significant differences. Therefore, we are as yet reluctant to consider the rock as an intrusive lamproite until further detailed mineralogical studies of this complex have been undertaken.

Acknowledgements

This research was supported by the Natural Sciences and Engineering Research Council of Canada, Lakehead University and the USSR Academy of Sciences. Ron Chapman is thanked for assistance with the electron microprobe work at the University of Manitoba and Alan MacKenzie for help with the SEM-EDS study and photographic work undertaken at Lakehead University.

References

Anderson, A. T. (1984) Probable relations between plagioclase zoning and magma dynamics, Fuego Volcano, Guatemala. *Am. Mineral.*, **69**, 660–76.

Bilibina, T. V., Daskova, A. D., Donakov, V. I., Titov, V. K., and Shchukin, S. N. (1967) *Petrologiya shchelochnogo vulkanogenno-intrutruzivnogo kompleksa Aldanskogo shchita* (*Petrology of the Alkaline Volcanic Intrusive Complexes of the Aldan Shield*). Nedra Press, Leningrad.

Bottinga, T., Kudo, A., and Weill, D. (1966) Some observations on oscillatory zoning and crystallization of magmatic plagioclase. *Am. Mineral.*, **51**, 792–806.

Drake, M. J. and Weill, D. F. (1972) New rare earth element standards for electron microprobe analysis. *Chem. Geol.*, **59**, 323–30.

Haggerty, S. E. and Mariano, A. N. (1983) Strontian loparite and strontio-chevkinite: Two new minerals in rheomorphic fenites from the Parana Basin carbonatites, South America. *Contrib. Mineral. Petrol.*, **84**, 365–81.

Lazebnik, K. A., Makhotko, V. F., and Lazebnik, Y. D. (1985) Pyervaya nakhodka praiderita v Vostochnoi Sibiri. (First occurence of priderite in Eastern Siberia). *Mineral. Zhurn.*, 7, 81–3.

Mitchell, R. H. (1993*a*) Accessory rare earth, strontium, barium and zirconium minerals in the Benfontein and Wesselton calcite kimberlites, South Africa. *Proc. 5th Internat. Kimberlite Conf.* (Meyer, H. O. A. and Leonardos, O. H., eds.). Companhia de Pesquisa de Recursos Minerais, Rio de Janeiro, Brazil. in press.

——(1993*b*) Suggestions for revisions to the terminology of kimberlites and lamprophyres from a genetic viewpoint. Ibid.

——and Bergman (1991) *Petrology of Lamproites*. Plenum Press, New York.

——and Meyer, H. O. A. (1989) Niobian K–Ba–V titanates from micaceous kimberlite, Star Mine, Orange Free State, South Africa. *Mineral. Mag.*, **53**, 451–6.

——and Steele, I. (1992) Zirconium and potassium silicates and strontian cerian perovskite in lamproites from the Leucite Hills, Wyoming, *Can. Mineral.*, **30**, 1153–9.

Myrha, S., White, T. J., Kesson, S. E., and Riviere, J. C., (1988) X-ray photoelectron spectroscopy for the direct identification of Ti valance in $[Ba_xCs_y][(Ti, Al)_{2x+y}Ti_{8-2x-y}]O_{16}$ hollandites. *Am. Mineral.*, **73**, 161–7.

Orlova, M. P. (1987) Novyye dannyye po geologii Malomurunskogo shchelochnogo massiva, yugo-zapadnaya Yakutiya. (Recent finding on the geology of the Little Murun alkaline massif, south western Yakutia). *Sovyetskaya Geologiya 1987*, 83–92. [Translated as *Internat. Geol. Review 1988*, **30**, 945–53].

——(1988) Petrokhimicheskiye osobennosti Malomurunskogo shchelochnogo massive, yugo-zapadnaya Yakutiya. (Petrochemistry of the Little Murun alkaline massif, south western Yakutia). *Izvestiya Akad. Nauk. SSSR., Ser. Geol. 1988*, 15–27. [Translated as *Internat. Geol Review, 1988*, **30**, 954–69].

Ritter, J. J., Roth, R. S., and Blendell, J. E. (1986) Alkoxide precursor synthesis and characterization of phases in the barium-titanium oxide system. *J. Am. Ceram. Soc.*, **69**, 155–62.

Shadenkov, Y. M., Orlova, M. P. and Borisov, A. B.

(1989) Piroksenity i shonkinity Malomurunskogo massivaintruzivnyye analogi lamproitov. (Pyroxenites and shonkinites of the Little Murun massif–intrusive analogues of lamproite). *Zap. Vses. Mineral. Obshch.*, **118**, 28–37. [Translated as *Internat. Geol. Review* 1990, **32**, 61–9].

Smyslov, S. A. (1986) Kalsilitsoderzhashchiye porody Malomurunskogo massiva. (Kalsilite-bearing rocks of the Little Murun massif). *Geologiya i Geofizika*, 33–38.

Tillmans, E. (1969) The crystal structure of $BaTi_5O_{11}$. *Acta Crystallogr. Sect. B*, **25B**, 1444–52.

Vladykin, N. V. (1985) Pyervaya nakhodka lamproitov v SSSR. (First occurrence of lamproite in the USSR.) *Dokl. Akad. Nauk SSSR*, **280**, 718–22.

——Matveyeva, L. H., Bogacheva, H. G., and Alekseyev, Y. A. (1983) Novyye danyye o charoite i charoitivykh porodakh. (Recent findings on charoite and charoitic rocks). In *Mineralogiya i Genezis Tsvetnikh Kamnei Vostochnoi Sibiri* (*Mineralogy and Genesis of Gem Stones of Eastern Siberia*), 41–56. Siberian Division Akad. Nauk. SSSR, Novosibirsk.

Vorobyev, E. I., Konyev, A. A., Malyshok, Y. V., Afonina, G. F. and Sapozhnikov, A. N. (1984) Tausonit $SrTiO_3$, novyye mineraly v perovskit gryppa. (Tausonite $SrTiO_3$, a new mineral of the perovskite group). *Zap. Vses. Mineral. Obshch.*, **113**, 83–9.

——————and Paradina, L. F. (1987) Tausonit, geologicheskiye usloviya abrazovaniya i mineralnii paragenezisi. (*Tausonite, geological conditions of formation and mineral paragenesis*). Nauka Press. Novosibirsk.

Zhuravleva, L. N., Yukina, K. V., and Ryabeva, E. G. (1978) Praiderit, Pyervaya nakhodka v SSSR. (Priderite, first find in the USSR). *Dokl. Akad. Nauk SSSR*, **239**, 435–8. (Translated as *Dokl. Akad. Nauk SSSR* **239**, 141–3.)

[*Manuscript received 6 May 1992: revised 23 October 1992*]